J. Phys. B: At. Mol. Opt. Phys. **21** (1988) 749-767. Printed in the UK

The influence of core fine-structure interactions on dielectronic recombination at low temperatures: B-like C, N and O recombined ions

N R Badnell†

Department of Applied Mathematics and Theoretical Physics, Silver Street, Cambridge, CB3 9EW, UK

Received 3 August 1987

Abstract. We use the program AUTOSTRUCTURE to calculate configuration-mixing intermediate-coupling effective dielectronic recombination rate coefficients for the recombined ions C^+, N^{2+} and O^{3+} at temperatures $T = 10^3$-6.3×10^4 K. We tabulate results for the quartet-quartet transition lines—these do not arise in *LS* coupling at low densities applicable to gaseous nebulae—as well as selected doublet-doublet lines. We also compare total rate coefficients for both direct radiative recombination and dielectronic recombination, the latter being calculated in both *LS* and intermediate coupling.

We find that core fine-structure interactions give rise to a number of new dielectronic recombination lines, a number of which are comparable in strength to all but the strongest *LS*-allowed lines and they also cause an increase in the total dielectronic recombination rate coefficient at $T = 10^4$ K of 12, 35 and 70% for C^+, N^{2+} and O^{3+} respectively. However, they are not strong enough for the weak interaction approximation of Nussbaumer and Storey to be applicable.

1. Introduction

Dielectronic recombination via the full Rydberg series of autoionising levels was shown by Burgess (1964) to be the dominant electron-ion recombination process at coronal temperatures. More recently it was suggested by Beigman and Chichkov (1980) and Harrington *et al* (1980) that dielectronic recombination via the core excitation of levels lying below the first dipole-excited level could be important at the low temperatures found in gaseous nebulae. This was confirmed by Beigman and Chichkov (1980) and Storey (1981). Since then Nussbaumer and Storey have calculated effective dielectronic recombination rate coefficients for ions of C, N, O (Nussbaumer and Storey 1984) Mg, Al, Si (Nussbaumer and Storey 1986) and Ne (Nussbaumer and Storey 1987) over $T = 10^3$-6×10^4 K.

The first calculations were carried out in *LS* coupling (Storey 1981, Nussbaumer and Storey 1983, 1984). However, core fine-structure interactions, and in particular spin-orbit interactions, mix *LS*-allowed and *LS*-forbidden autoionising levels, giving access to *LS*-allowed radiative channels that were formerly inaccessible. The mixing need not be large (in fact it is not) since *LS*-allowed autoionisation transition rates (A_a) are many orders of magnitude greater than the corresponding radiative rates (A_r).

† Present address: Department of Physics, Auburn University, Auburn, Alabama 36849, USA.

0953-4075/88/050749+19$02.50

As a result, Nussbaumer and Storey (1984) introduced a weak interaction (WI) approximation to try to allow for this effect. Radiative rates were still calculated in *LS* coupling but it was assumed that the core fine-structure interactions were strong enough so that $A_a \gg A_r$ for all terms forbidden to autoionise in *LS* coupling. This WI approximation provides an upper bound for the recombination coefficients while the original *LS*-coupling approximation provides a lower bound. A more refined treatment (Nussbaumer and Storey 1986, 1987) used one or other of the two approximations for each autoionising term depending on the *LS*-coupling ratio A_a^{LS}/A_r^{LS} and the strength of the core fine-structure interaction. The accuracy of this approach thus depends on the judicious use of one or other of the two limiting approximations, but of course in the case of $A_a^{IC} \sim A_r^{IC}$ neither limiting approximation is valid.

With this in mind we use the program AUTOSTRUCTURE (see Badnell 1985, 1986 and later in this paper) to carry out an explicit intermediate-coupling calculation for C^+, N^{2+}, O^{3+} recombined ions at temperatures $T = 10^3$-6.3×10^4 K. The B-like recombined ions provide an extreme example, since if we assume that only the ground term of the Be target ion is populated (applicable to gaseous nebulae) then the quartet-quartet autoionising levels are only populated via core fine-structure interactions. The subsequent radiative cascade is well described by *LS* coupling (i.e. doublet-quartet radiative transition rates are neglible) so the effective dielectronic recombination rate coefficients for quartet-quartet transition lines are totally dependent on the initial populating mechanism—core fine-structure interactions. The $^2S^\circ$, $^2D^\circ$, ... and ^2P, ^2F, ... terms are also forbidden to autoionise to the ^1S ground term in *LS* coupling due to parity conservation.

In § 2 we briefly describe the theory behind the calculation, in § 3 we discuss our use of the Breit-Pauli Hamiltonian and in § 4 we outline further developments of the AUTOSTRUCTURE program and describe its application to B-like recombined ions. In § 5 we present tables of results for effective dielectronic recombination rate coefficients for quartet-quartet transition lines and selected doublet-doublet lines and compare total *LS*-coupling and intermediate-coupling dielectronic recombination rate coefficients and direct radiative recombination rate coefficients for B-like C, N and O recombined ions for $T = 10^3$-10^5 K. Also, the tables of total dielectronic recombination rate coefficients of Badnell (1987a) are extended to low temperatures for these ions.

2. Theory

The formulation of the dielectronic recombination problem has been given by Burgess (1966) and it has been discussed by Nussbaumer and Storey (1983, 1984) in connection with low temperatures, and so we present only a brief discription.

2.1. Effective dielectronic recombination rate coefficients

Consider an ion X^{z+} whose states are populated by dielectronic capture and subsequent radiative cascade. We may define an effective dielectronic recombination rate coefficient $\alpha_d^*(i;j)$ for a state j and an effective dielectronic recombination rate coefficient $\alpha_d^*(i;j \to h)$ for a transition line $j \to h$ such that

$$N_e N(X_i^{(z+1)+}) \alpha_d^*(i;j) \tag{2.1}$$

is the total number of ions X_j^{z+} formed in a state j per unit volume per unit time from

an initial ion $X_i^{(z+1)+}$ in a state i and

$$N_e N(X_i^{(z+1)+}) \alpha_d^*(i; h \to j) \tag{2.2}$$

is the total number of photons emitted in the transition line $h \to j$ per unit volume per unit time, again from an initial ion state i. N_e is the electron number density and $N(X_i^{(z+1)+})$ is the number density of the initial ion $X_i^{(z+1)+}$ in a state i. At electron densities applicable to gaseous nebulae (typically $N_e \sim 10^4$ cm^{-3}) we assume the initial population to be concentrated in the ground state $i = g$. We thus drop the explicit dependence on i from our notation, namely $\alpha_d^*(j)$ and $\alpha_d^*(h \to j)$. In LS coupling g is the ground term and in intermediate coupling g is the ground level. Differences can arise between LS-coupling and intermediate-coupling results for α_d^* if the initial ground term contains more than one level and A_a^{IC} is not independent of J for a given SL term.

If j is bound

$$\alpha_d^*(j) = \sum_{h>j} \alpha_d^*(h \to j) \tag{2.3}$$

where

$$\alpha_d^*(h \to j) = \frac{A_r(h \to j)}{\Sigma_{k<h} A(h \to k)} \alpha_d^*(h) \tag{2.4}$$

and the sum of transition probabilities in the denominator of (2.4) contains both radiative (A_r) and, if energetically possible, autoionisation (A_a) rates.

If j is autoionising

$$\alpha_d^*(j) = R_S(g; j) \sum_l A_a(j \to g, E_c l) + \sum_{h>j} \alpha_d^*(h \to j) \tag{2.5}$$

and R_S is given by the Saha-Boltzman equation

$$R_S(g; j) = \left(\frac{N(X_j^{z+})}{N_e N(X_g^{(z+1)+})} \right)_S = \frac{\omega(j)}{2\omega(g)} \times \left(\frac{4\pi a_0^2 I_H}{kT} \right)^{3/2} \exp(-E_c/kT) \tag{2.6}$$

where E_c is the energy (in Ryd) of the continuum electron which is fixed by the position of the resonances, $\omega(j)$ is the statistical weight of the $(N+1)$-electron intermediate state, $\omega(g)$ is the statistical weight of the N-electron target ion and $(4\pi a_0^2 I_H/k)^{3/2} = 4.1414 \times 10^{-16}$ cm^3.

The second term in (2.5) can be neglected in LS coupling (see Nussbaumer and Storey 1983) since in general $A_a^{LS} \gg A_r^{LS}$; we need to re-examine this point in intermediate coupling. However, due to the exponential temperature cut-off in (2.6) radiative transitions between autoionising levels could only be important at the highest temperatures we consider. Finally, the total dielectronic recombination rate coefficient $\alpha_d(\text{tot})$ for the given initial state g is just $\alpha_d^*(j)$ summed over the ground and metastable states j.

2.2. Transition probabilities

Configuration mixing LS- and intermediate-coupling autoionisation transition rates are evaluated by AUTOSTRUCTURE according to equations (2.2) and (2.4) of Badnell (1986) respectively. In the original version of AUTOSTRUCTURE as described by Badnell (1985, 1986) the continuum orbital was only approximately evaluated at the energy given by the conservation equation (2.5) of Badnell (1986). The resulting error was

negligible for $\Delta n_c > 0$ core transitions. The continuum orbitals are now evaluated at three user-supplied energies, chosen so as to span the range of interest, and a three-point Lagrange interpolation formula is used to evaluate the bound-continuum Slater and one-body integrals at the energy given by the conservation equation.

Configuration mixing *LS*- and intermediate-coupling electric-dipole radiative transition rates can be evaluated as described by Eissner *et al* (1974) since AUTOSTRUCTURE incorporates the program SUPERSTRUCTURE. However, there is no need to evaluate the full intermediate-coupling line strength given by Eissner *et al* (1974, equation (117)); it is sufficient and very much faster to evaluate

$$S^{[1]}(\Gamma SLJ, \Gamma' S'L'J')$$

$$= |\langle \Gamma SLJ \,|\, C\beta SLJ\rangle\langle C\beta SLJ \| P^{[1]} \| C'\beta' S'L'J'\rangle\langle C'\beta' S'L'J' \,|\, \Gamma' S'L'J'\rangle|^2 \qquad (2.7)$$

in the notation of Eissner *et al* (1974), where the selection rules $S = S'$, $|L - L'| \leqslant 1$ ($L' = 0 = L$ forbidden) and $|J - J'| \leqslant 1$ ($J' = 0 = J$ forbidden) apply and the reduced matrix element in (2.7) is given by Eissner *et al* (1974, equation (116)).

Radiative rates evaluated using equation (2.7) differ by less than 1% from those evaluated using equation (117) of Eissner *et al* (1974) for all but the very weakest transitions. Also, the radiative transitions that are forbidden by the selection rules operating with (2.7) still have negligible rates when the full intermediate-coupling selection rules operate (typically a factor of 10^6 smaller than the strongest radiative rates).

3. The Breit–Pauli Hamiltonian

This was derived by Bethe and Salpeter (see e.g. their 1977 reprint) and it is discussed in detail by Jones (1970, 1971) and so we discuss it only in relation to the problem at hand.

3.1. The relativistic two-body terms

The Breit–Pauli Hamiltonian as implemented by SUPERSTRUCTURE (see Eissner *et al* 1974) contains all of the relativistic one-body terms and the two-body fine-structure terms while the two-body non-fine-structure terms are neglected. The omission of the orbit–orbit, contact spin–spin and two-body Darwin operators is unlikely to cause any serious error since they commute with $\boldsymbol{L}^2$ and $\boldsymbol{S}^2$ and so do not mix distinct *SL* terms, which is what we are particularly interested in. The two-body spin–orbit and spin–other-orbit interactions consist of interactions between valence electrons and of interactions between valence electrons and closed-shell electrons (see Blume and Watson 1962), while the spin–spin interactions arise only between valence electrons.

We have investigated the relative importance of the various contributions to the two-body fine-structure interactions in the case of the 2s2p4*l* autoionising levels of N^{2+}. Restricting interactions between valence electrons to within a single configuration changes the autoionisation rates by less than 5%, and often much less. Furthermore, neglecting all interactions between valence electrons changes all but the weakest *LS*-forbidden A_a by less than 10% in general. This should be compared with errors in general of ±30% that can arise on using different configuration expansions. Further-

more, the effect on $\alpha_d^*(j \to h)$ for individual $J \to J'$ LS-forbidden transitions is generally only one or two per cent. However, we do retain the interactions between valence electrons and closed-shell electrons and these give rise to terms similar to the one-body nuclear spin–orbit term and these are incorporated into a generalised spin–orbit parameter (see Eissner *et al* 1974). Also, the one-body Darwin and mass variation terms are included in full.

To sum up, we have neglected all (relativistic) two-body interactions of the Breit–Pauli Hamiltonian that cannot be incorporated into a generalised spin–orbit parameter. For higher-Z ions, the Z^3 dependence of the one-body interactions compared with the Z^2 dependence of the two-body interactions would have led us to this approach.

3.2. Term energy corrections

Jones (1971) noted that small errors in non-relativistic energies could lead to much larger errors in fine-structure splittings. Zeippen *et al* (1977) thus introduced a semi-empirical correction to the non-relativistic Hamiltonian; namely if we have $\boldsymbol{V}$ such that $\boldsymbol{V}\boldsymbol{H}_{nr}\boldsymbol{V}^T = \boldsymbol{E}_{nr}$, then choose $\boldsymbol{D}$, a set of term energy corrections to the non-relativistic energies, take $\boldsymbol{H}'_{BP} = \boldsymbol{H}_{nr} + \boldsymbol{H}_D + \boldsymbol{H}_{rc}$ and solve $\boldsymbol{U}\boldsymbol{H}'_{BP}\boldsymbol{U}^T = \boldsymbol{E}'_{BP}$ where $\boldsymbol{H}_D = \boldsymbol{V}^T\boldsymbol{D}\boldsymbol{V}$, $\boldsymbol{H}_{nr}$ is the non-relativistic Hamiltonian and $\boldsymbol{H}_{rc}$ is the relativistic correction (see Eissner *et al* 1974). We choose $\boldsymbol{D}$ such that $\boldsymbol{E}'_{BP}$ best agrees with the observed energy levels in Moore (1970, 1975, 1983). Uncertainties in the position of the unobserved autoionising levels give rise to errors in the temperature dependence of $\alpha_d^*(j \to k)$ for transitions from these levels and for subsequent cascades (see equation (2.6)).

4. Application to B-like recombined ions

We include the following configurations in our calculations (the $1s^2$ core has been suppressed):

$2s^22p$,	$2s2p^2$,	$2p^3$	
$2s^2nl$,	$2s2pnl$,	$2p^2nl$	$l < n, 3 \leqslant n \leqslant n_0$
$2s^2kl$,	$2s2pkl$,	$2p^2kl$	$l \leqslant 6$
$2s^2\overline{4l}$,	$2s2p\overline{4l}$,	$2p^2\overline{4l}$	$\bar{l} \leqslant 2$

where kl denotes a continuum orbital, $\overline{4l}$ a correlation orbital, $n_0 = 5$ for C^+ and N^{2+} and $n_0 = 6$ for O^{3+}. The lowest autoionising levels arise from the $2s2p3l$ and $2s2p4l$ configurations for C^+ and N^{2+} respectively and from the $2p^23l$ and $2s2p5l$ configurations for O^{3+}. Levels with $n > n_0$ are dealt with by extrapolation, see § 5.

The original AUTOSTRUCTURE code (see Badnell 1985, 1986) used only l-dependent model potentials. Following Nussbaumer and Storey (1978) that restriction has been removed. We use bound spectroscopic orbitals nl evaluated in a Thomas–Fermi model potential with radial scaling parameters λ_{nl} and we use bound correlation orbitals evaluated in a screened hydrogenic potential.

The spectroscopic λ_{nl} were determined by minimising the weighted sum of all eigenenergies of the spectroscopic terms of the B-like recombined ion. The nl spectroscopic orbitals were orthonormalised at each step of the variation to all other spectroscopic orbitals $n'l'$, such that $n' < n$ and $l' = l$. The correlation screening parameters

were determined by minimising a sum of spectroscopic eigenenergies subject to the orthonormalisation of the $\overline{nl}$ correlation orbitals to all of the nl spectroscopic orbitals with $l = \bar{l}$ (the spectroscopic orbitals remain unchanged). The $\overline{nl}$ correlation orbitals have a mean radius between those of the $n = 2$ and 3 orbitals and are included to improve the structure of the 2:2:2 and 2:2:3 complexes (see Nussbaumer and Storey 1981). λ_{nl} were determined for $nl = 1s, \ldots, 4f$ and we then took $\lambda_{nl} = \lambda_{4l}$ for $n > 4$ and $\lambda_{nl} = \lambda_{4f}$ for $l \geqslant 3$. The Be target uses the same 1s, 2s and 2p orbitals as for the B-like ion (as all rates A_a and A_r are evaluated at the same time) and the eigenenergies relative to the ground 2^1S term differ by less than or equal to 1% from those evaluated by minimising Be term energies.

We also tried using a different model potential, one based on Slater-type orbitals (STO) due to Burgess (private communication). After minimisation, the B-like eigenenergies differed little (<1%) from those obtained using the Thomas–Fermi model potential, although the scaling parameters were closer to unity (unscaled). An option to use an STO model potential in place of the Thomas–Fermi one has been incorporated into the AUTOSTRUCTURE code.

We evaluated the continuum orbitals kl at the interpolation energies according to the same prescription as for highly excited nl spectroscopic orbitals of the B-like ion. Namely, we used the same Thomas–Fermi model potential as for the $n_0 l$ orbital and orthogonalised the resulting continuum orbital to all spectroscopic orbitals of the same orbital angular momentum. The kl continuum orbital is of course automatically orthogonal to both the $4l$, $5l$ and, if included, $6l$ orbitals.

5. Results

In tables 1–3 we present our results for intermediate-coupling effective dielectronic recombination rate coefficients for C^+, N^{2+} and O^{3+} over the range $T = 10^3$–6.3×10^4 K. In table 4 we present our intermediate-coupling results for the total dielectronic recombination rate coefficient α_d(tot). In figures 1–3 we compare our *LS*-coupling

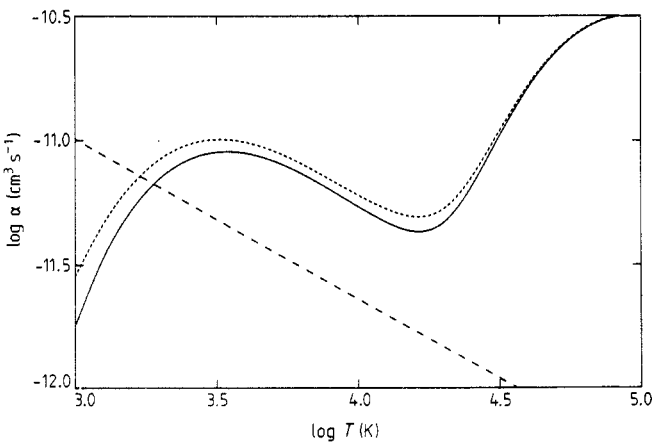

Figure 1. Total recombination rate coefficients for C^+. ——, *LS*-coupling dielectronic recombination, this work; - - - -, intermediate-coupling dielectronic recombination, this work; – – –, direct radiative recombination, Aldrovandi and Péquignot (1973).

Table 1. Effective dielectronic recombination rate coefficients for C^+ ($cm^3 s^{-1}$).

							log (T)									
λ (Å)	$2S'+1$	L'	$2S'+1$	L	E_i	E_k	3.0	3.2	3.4	3.6	3.8	4.0	4.2	4.4	4.6	4.8
7079.1	4	2	−4	3	181 634	195 760	7.27 (−24)†	5.73 (−20)	1.56 (−17)	6.17 (−16)	6.47 (−15)	2.61 (−14)	5.52 (−14)	7.43 (−14)	7.25 (−14)	5.65 (−14)
6838.9	−4	1	4	2	167 011	181 634	1.90 (−16)	3.21 (−16)	8.53 (−16)	4.95 (−15)	1.93 (−14)	4.90 (−14)	8.51 (−14)	1.05 (−13)	9.91 (−14)	7.57 (−14)
6101.3	2	1	−2	2	181 999	198 389	2.49 (−14)	3.19 (−14)	2.90 (−14)	2.11 (−14)	1.35 (−14)	8.05 (−15)	4.80 (−15)	2.94 (−15)	1.81 (−15)	1.10 (−15)
5157.9	−4	1	4	1	167 011	186 399	3.08 (−16)	5.09 (−16)	9.86 (−16)	4.02 (−15)	1.08 (−14)	1.73 (−14)	2.04 (−14)	1.97 (−14)	1.61 (−14)	1.14 (−14)
4416.4	−2	2	2	3	198 389	221 032	3.00 (−27)	6.39 (−22)	1.14 (−18)	9.93 (−17)	1.29 (−15)	5.09 (−15)	9.43 (−15)	1.09 (−14)	9.26 (−15)	6.51 (−15)
4376.5	−4	1	4	2	198 814	221 664	2.56 (−27)	7.68 (−22)	1.70 (−18)	1.70 (−16)	2.40 (−15)	9.95 (−15)	1.90 (−14)	2.21 (−14)	1.89 (−14)	1.33 (−14)
4318.3	4	1	−4	1	186 399	209 557	2.59 (−20)	1.23 (−17)	4.65 (−16)	3.58 (−15)	1.01 (−14)	1.51 (−14)	1.51 (−14)	1.18 (−14)	7.80 (−15)	4.67 (−15)
4076.6	−4	2	4	3	196 516	221 046	5.39 (−27)	1.16 (−21)	2.07 (−18)	1.81 (−16)	2.37 (−15)	9.41 (−15)	1.77 (−14)	2.07 (−14)	1.79 (−14)	1.27 (−14)
3880.2	−4	3	4	4	195 760	221 532	5.42 (−27)	1.50 (−21)	3.15 (−18)	3.05 (−16)	4.24 (−15)	1.74 (−14)	3.30 (−14)	3.86 (−14)	3.32 (−14)	2.34 (−14)
3581.3	4	2	−4	1	181 634	209 557	2.86 (−20)	1.36 (−17)	5.14 (−16)	3.95 (−15)	1.11 (−14)	1.67 (−14)	1.67 (−14)	1.30 (−14)	8.61 (−15)	5.15 (−15)
2796.3	−4	3	4	4	195 760	231 521	1.82 (−33)	1.01 (−25)	6.03 (−21)	4.81 (−18)	2.53 (−16)	2.39 (−15)	7.63 (−15)	1.23 (−14)	1.29 (−14)	1.03 (−14)
2637.6	4	2	−4	3	181 634	219 547	1.77 (−26)	1.71 (−21)	1.85 (−18)	1.18 (−16)	1.30 (−15)	4.85 (−15)	9.35 (−15)	1.18 (−14)	1.10 (−14)	8.31 (−15)
1335.4	−2	1	2	2	0	74 886	2.45 (−12)	5.89 (−12)	8.34 (−12)	8.17 (−12)	6.33 (−12)	4.36 (−12)	3.01 (−12)	2.21 (−12)	1.66 (−12)	1.19 (−12)
1139.2	2	1	−2	2	110 608	198 389	2.60 (−13)	3.33 (−13)	3.02 (−13)	2.20 (−13)	1.41 (−13)	8.41 (−14)	5.01 (−14)	3.07 (−14)	1.89 (−14)	1.15 (−14)
909.3	2	1	−2	2	110 608	220 585	6.56 (−27)	1.10 (−21)	1.70 (−18)	1.35 (−16)	1.66 (−15)	6.33 (−15)	1.16 (−14)	1.33 (−14)	1.13 (−14)	8.02 (−15)
904.1	−2	1	2	1	0	110 608	2.68 (−13)	3.99 (−13)	5.05 (−13)	5.45 (−13)	4.87 (−13)	3.95 (−13)	3.37 (−13)	3.09 (−13)	2.75 (−13)	2.21 (−13)
809.7	2	2	−2	2	74 886	198 389	7.38 (−13)	9.47 (−13)	8.59 (−13)	6.26 (−13)	3.99 (−13)	2.39 (−13)	1.42 (−13)	8.71 (−14)	5.38 (−14)	3.25 (−14)
806.4	4	1	−4	1	42 997	167 011	1.36 (−15)	2..22 (−15)	3.36 (−15)	1.07 (−14)	3.30 (−14)	7.13 (−14)	1.12 (−13)	1.32 (−13)	1.21 (−13)	9.09 (−14)
799.8	2	2	−2	3	74 886	199 922	1.70 (−12)	4.92 (−12)	7.44 (−12)	7.49 (−12)	5.83 (−12)	3.86 (−12)	2.30 (−12)	1.29 (−12)	6.93 (−13)	3.63 (−13)
686.3	2	2	−2	2	74 886	220 585	2.30 (−26)	3.86 (−21)	5.94 (−18)	4.72 (−16)	5.81 (−15)	2.22 (−14)	4.05 (−14)	4.65 (−14)	3.97 (−14)	2.81 (−14)
651.4	4	1	−4	2	42 997	196 516	2.49 (−24)	2.83 (−20)	1.05 (−17)	4.56 (−16)	4.63 (−15)	1.78 (−14)	3.62 (−14)	4.76 (−14)	4.58 (−14)	3.53 (−14)
641.8	4	1	−4	1	42 997	198 814	6.71 (−14)	1.08 (−13)	1.13 (−13)	9.07 (−14)	6.36 (−14)	4.86 (−14)	4.61 (−14)	4.51 (−14)	3.87 (−14)	2.84 (−14)
600.4	4	1	−4	1	42 997	209 557	9.12 (−20)	4.32 (−17)	1.64 (−15)	1.26 (−14)	3.55 (−14)	5.31 (−14)	5.33 (−14)	4.14 (−14)	2.75 (−14)	1.64 (−14)
564.7	4	1	−4	2	42 997	220 097	4.87 (−26)	6.33 (−21)	8.27 (−18)	5.94 (−16)	6.90 (−15)	2.57 (−14)	4.72 (−14)	5.54 (−14)	4.85 (−14)	3.49 (−14)
562.5	4	1	−4	1	42 997	220 773	5.09 (−27)	9.49 (−22)	1.56 (−18)	1.30 (−16)	1.68 (−15)	6.90 (−15)	1.39 (−14)	1.78 (−14)	1.67 (−14)	1.27 (−14)
549.5	−2	1	2	1	0	181 999	1.91 (−14)	2.70 (−14)	3.11 (−14)	3.17 (−14)	2.97 (−14)	2.65 (−14)	2.26 (−14)	1.81 (−14)	1.34 (−14)	9.18 (−15)
532.7	4	1	−4	2	42 997	230 717	1.20 (−32)	4.38 (−25)	2.00 (−20)	1.35 (−17)	6.39 (−16)	5.65 (−15)	1.73 (−14)	2.72 (−14)	2.80 (−14)	2.21 (−14)
446.4	−2	1	2	1	0	214 405	5.81 (−23)	3.67 (−19)	7.12 (−17)	1.53 (−15)	8.24 (−15)	1.85 (−14)	2.40 (−14)	2.19 (−14)	1.61 (−14)	1.03 (−14)
			$2S+1$	L	$2J$	E_j	3.0	3.2	3.4	3.6	3.8	4.0	4.2	4.4	4.6	4.8
			−2	1	1	0	7.25 (−13)	1.94 (−12)	2.95 (−12)	3.08 (−12)	2.53 (−12)	1.88 (−12)	1.45 (−12)	1.24 (−12)	1.08 (−12)	8.87 (−13)
			−2	1	3	63	2.06 (−12)	4.62 (−12)	6.58 (−12)	6.67 (−12)	5.40 (−12)	3.96 (−12)	3.01 (−12)	2.52 (−12)	2.18 (−12)	1.77 (−12)
			4	1	1	43 001	2.41 (−14)	3.90 (−14)	4.16 (−14)	3.93 (−14)	4.59 (−14)	6.80 (−14)	9.88 (−14)	1.17 (−13)	1.10 (−13)	8.41 (−14)
			4	1	3	43 024	1.72 (−14)	2.78 (−14)	3.01 (−14)	3.13 (−14)	4.38 (−14)	7.20 (−14)	1.07 (−13)	1.27 (−13)	1.18 (−13)	9.05 (−14)
			4	1	5	43 063	2.72 (−14)	4.38 (−14)	4.68 (−14)	4.47 (−14)	5.69 (−14)	9.54 (−14)	1.46 (−13)	1.75 (−13)	1.62 (−13)	1.23 (−13)

† 7.27 (−24) = 7.27×10^{-24}.

Table 2. Effective dielectronic recombination rate coefficients for N^{2+} ($cm^3 s^{-1}$).

							log (T)									
λ (Å)	$2S'+1$	L'	$2S'+1$	L	E_i	E_k	3.0	3.2	3.4	3.6	3.8	4.0	4.2	4.4	4.6	4.8
13 918.7	4	2	−4	3	376 749	383 933	3.17 (−14)†	3.20 (−14)	2.50 (−14)	1.66 (−14)	1.00 (−14)	5.96 (−15)	3.91 (−15)	2.99 (−15)	2.37 (−15)	1.73 (−15)
6 937.6	2	2	−2	3	373 252	387 667	2.02 (−15)	1.50 (−14)	4.11 (−14)	6.03 (−14)	5.94 (−14)	4.57 (−14)	3.00 (−14)	1.78 (−14)	9.95 (−15)	5.34 (−15)
4 864.0	4	2	−4	3	309 659	330 218	5.98 (−14)	4.08 (−13)	1.19 (−12)	1.83 (−12)	1.88 (−12)	1.51 (−12)	1.07 (−12)	7.41 (−13)	5.04 (−13)	3.29 (−13)
4 519.7	−4	1	4	2	287 533	309 659	1.16 (−12)	1.54 (−12)	2.08 (−12)	2.43 (−12)	2.25 (−12)	1.76 (−12)	1.28 (−12)	9.53 (−13)	6.99 (−13)	4.81 (−13)
4 414.7	4	2	−4	3	388 198	410 850	2.06 (−29)	3.41 (−23)	2.23 (−19)	4.40 (−17)	9.58 (−16)	5.18 (−15)	1.17 (−14)	1.51 (−14)	1.37 (−14)	1.00 (−14)
4 226.9	4	3	−4	4	386 881	410 540	4.35 (−29)	6.07 (−23)	3.54 (−19)	6.52 (−17)	1.36 (−15)	7.15 (−15)	1.58 (−14)	2.02 (−14)	1.83 (−14)	1.33 (−14)
4 146.1	4	2	−4	1	376 749	400 868	1.54 (−23)	1.22 (−19)	2.72 (−17)	6.39 (−16)	3.63 (−15)	8.43 (−15)	1.11 (−14)	1.02 (−14)	7.54 (−15)	4.82 (−15)
4 075.4	−4	1	4	2	386 150	410 688	3.11 (−29)	4 74 (−23)	2.92 (−19)	5.58 (−17)	1.19 (−15)	6.35 (−15)	1.42 (−14)	1.82 (−14)	1.65 (−14)	1.21 (−14)
4 029.0	−4	2	4	3	385 188	410 008	1.02 (−28)	1.07 (−22)	5.22 (−19)	8.59 (−17)	1.67 (−15)	8.40 (−15)	1.80 (−14)	2.27 (−14)	2.03 (−14)	1.46 (−14)
3 763.9	−4	1	4	0	287 533	314 101	2.15 (−15)	7.67 (−15)	1.41 (−14)	1.66 (−14)	1.51 (−14)	1.26 (−14)	1.09 (−14)	1.02 (−14)	8.77 (−15)	6.64 (−15)
3 731.3	−4	3	4	4	383 933	410 734	5.26 (−29)	7.98 (−23)	4.91 (−19)	9.36 (−17)	1.99 (−15)	1.06 (−14)	2.37 (−14)	3.05 (−14)	2.77 (−14)	2.02 (−14)
3 389.3	2	2	−2	1	373 252	402 757	1.97 (−24)	4.41 (−20)	1.90 (−17)	6.76 (−16)	4.99 (−15)	1.37 (−14)	2.00 (−14)	1.97 (−14)	1.51 (−14)	9.90 (−15)
3 365.5	−4	1	4	1	287.533	317 247	4.28 (−14)	8.80 (−14)	1.09 (−13)	9.93 (−14)	7.85 (−14)	6.69 (−14)	6.74 (−14)	7.27 (−14)	6.77 (−14)	5.29 (−14)
2 199.2	−2	3	2	4	342 667	388 138	1.02 (−14)	9.74 (−14)	3.13 (−13)	5.08 (−13)	5.34 (−13)	4.57 (−13)	2.87 (−13)	1.73 (−13)	9.78 (−14)	5.28 (−14)
1 920.1	−4	1	4	2	336 117	388 198	1.62 (−14)	1.61 (−13)	5.30 (−13)	8.73 (−13)	9.27 (−13)	7.46 (−13)	5.05 (−13)	3.08 (−13)	1.75 (−13)	9.55 (−14)
1 908.2	−2	2	2	3	334 445	386 850	2.97 (−14)	1.42 (−13)	2.95 (−13)	3.63 (−13)	3.22 (−13)	2.33 (−13)	1.52 (−13)	9.61 (−14)	5.98 (−14)	3.63 (−14)
1 846.2	−4	2	4	3	332 717	386 881	7.24 (−14)	3.54 (−13)	7.45 (−13)	9.25 (−13)	8.22 (−13)	5.95 (−13)	3.85 (−13)	2.37 (−13)	1.43 (−13)	8.39 (−14)
1 802.4	−4	2	4	2	332 717	388 198	3.50 (−15)	3.48 (−14)	1.15 (−13)	1.89 (−13)	2.01 (−13)	1.62 (−13)	1.09 (−13)	6.66 (−14)	3.79 (−14)	2.07 (−14)
1 764.8	−4	3	4	3	330 218	386 881	7.38 (−15)	3.60 (−14)	7.59 (−14)	9.42 (−14)	8.38 (−14)	6.07 (−14)	3.93 (−14)	2.42 (−14)	1.45 (−14)	8.55 (−15)
1 730.3	−4	3	4	4	330 218	388 012	4.06 (−14)	3.58 (−13)	1.09 (−12)	1.71 (−12)	1.77 (−12)	1.39 (−12)	9.33 (−13)	5 63.(−13)	3.19 (−13)	1.74 (−13)

1 471.9	4	1	−4	2	317 247	385 188	4.04 (−14)	8.03 (−14)	9.61 (−14)	8.35 (−14)	5.93 (−14)	3.75 (−14)	2.28 (−14)	1.40 (−14)	8.72 (−15)	5.36 (−15)
1 346.4	4	2	−4	3	309 659	383 933	1.09 (−12)	1.10 (−12)	8.62 (−13)	5.73 (−13)	3.46 (−13)	2.05 (−13)	1.35 (−13)	1.03 (−13)	8.17 (−14)	5.98 (−14)
1 242.0	−4	3	4	4	330 218	410 734	1.37 (−28)	2.08 (−22)	1.28 (−18)	2.44 (−16)	5.18 (−15)	2.77 (−14)	6.17 (−14)	7.92 (−14)	7.19 (−14)	5.24 (−14)
991.0	−2	1	2	2	0	100 910	4.56 (−13)	2.69 (−12)	7.26 (−12)	1.14 (−11)	1.28 (−11)	1.19 (−11)	9.84 (−12)	7.82 (−12)	5.96 (−12)	4.25 (−12)
979.9	2	2	−2	2	100 910	202 963	8.44 (−15)	4.35 (−14)	1.01 (−13)	1.38 (−13)	1.41 (−13)	1.39 (−13)	1.69 (−13)	2.31 (−13)	2.69 (−13)	2.53 (−13)
773.1	2	2	−2	2	267 127	396 471	1.04 (−19)	8.32 (−17)	4.37 (−15)	4.13 (−14)	1.32 (−13)	2.13 (−13)	2.23 (−13)	1.79 (−13)	1.20 (−13)	7.30 (−14)
685.7	−2	1	2	1	0	145 841	2.50 (−14)	1.50 (−13)	4.83 (−13)	1.02 (−12)	1.79 (−12)	2.58 (−12)	3.00 (−12)	2.98 (−12)	2.54 (−12)	1.90 (−12)
434.1	4	1	−4	1	57 173	287 533	1.22 (−12)	1.65 (−12)	2.22 (−12)	2.57 (−12)	2.37 (−12)	1.87 (−12)	1.40 (−12)	1.08 (−12)	8.17 (−13)	5.72 (−13)
428.2	2	2	−2	2	100 910	334 445	2.43 (−14)	1.28 (−13)	2.97 (−13)	4.00 (−13)	3.81 (−13)	2.93 (−13)	2.06 (−13)	1.44 (−13)	1.01 (−13)	6.82 (−14)
399.0	2	1	−2	2	145 841	396 471	4.70 (−19)	3.76 (−16)	1.98 (−14)	1.87 (−13)	5.96 (−13)	9.62 (−13)	1.01 (−12)	8.07 (−13)	5.45 (−13)	3.30 (−13)
362.9	4	1	−4	2	57 173	332 717	7.86 (−14)	3.91 (−13)	8.61 (−13)	1.11 (−12)	1.03 (−12)	7.18 (−13)	5.50 (−13)	3.90 (−13)	2.77 (−13)	1.87 (−13)
358.5	4	1	−4	1	57 173	336 117	1.72 (−14)	1.61 (−13)	5.27 (−13)	8.67 (−13)	9.24 (−13)	7.56 (−13)	5.38 (−13)	3.62 (−13)	2.36 (−13)	1.47 (−13)
352.0	2	2	−2	2	100 910	385 030	1.25 (−13)	2.29 (−13)	2.59 (−13)	2.17 (−13)	1.51 (−13)	9.75 (−14)	6.41 (−14)	4.59 (−14)	3.38 (−14)	2.36 (−14)
348.7	2	2	−2	3	100 910	387 667	2.52 (−13)	1.87 (−12)	5.13 (−12)	7.52 (−12)	7.41 (−12)	5.70 (−12)	3.74 (−12)	2.22 (−12)	1.24 (−12)	6.66 (−13)
338.3	2	2	−2	2	100 910	396 471	1.38 (−19)	1.10 (−16)	5.79 (−15)	5.47 (−14)	1.75 (−13)	2.82 (−13)	2.96 (−13)	2.37 (−13)	1.60 (−13)	9.67 (−14)
304.9	4	1	−4	2	57 173	385 188	7.53 (−13)	1.50 (−12)	1.79 (−12)	1.56 (−12)	1.11 (−12)	7.00 (−13)	4.24 (−13)	2.61 (−13)	1.63 (−13)	9.99 (−14)
304.0	4	1	−4	1	57 173	386 150	4.47 (−14)	1.51 (−13)	2.51 (−13)	2.69 (−13)	2.19 (−13)	1.55 (−13)	1.09 (−13)	8.06 (−14)	6.02 (−14)	4.22 (−14)
284.3	4	1	−4	2	57 173	408 866	4.81 (−27)	2.77 (−21)	9.28 (−18)	1.20 (−15)	2.01 (−14)	9.20 (−14)	1.86 (−13)	2.25 (−13)	1.97 (−13)	1.40 (−13)

	$2S+1$	L	$2J$	E_j	3.0	3.2	3.4	3.6	3.8	4.0	4.2	4.4	4.6	4.8
	−2	1	1	0	2.38 (−13)	1.30 (−12)	3.50 (−12)	5.61 (−12)	6.61 (−12)	6.51 (−12)	5.76 (−12)	4.85 (−12)	3.86 (−12)	2.85 (−12)
	−2	1	3	173	3.07 (−13)	2.09 (−12)	6.18 (−12)	1.05 (−11)	1.31 (−11)	1.35 (−11)	1.22 (−11)	1.03 (−11)	8.17 (−12)	5.98 (−12)
	4	1	1	57 187	5.55 (−13)	1.00 (−12)	1.47 (−12)	1.66 (−12)	1.48 (−12)	1.15 (−12)	8.60 (−13)	6.66 (−13)	5.05 (−13)	3.55 (−13)
	4	1	3	57 248	5.44 (−13)	1.01 (−12)	1.53 (−12)	1.78 (−12)	1.61 (−12)	1.27 (−12)	9.60 (−13)	7.53 (−13)	5.78 (−13)	4.09 (−13)
	4	1	5	57 349	1.02 (−12)	1.84 (−12)	2.65 (−12)	2.94 (−12)	2.60 (−12)	2.01 (−12)	1.54 (−12)	1.24 (−12)	9.79 (−13)	7.05 (−13)

† 3.17 (−14)=3.17×10^{-14}.

Table 3. Effective dielectronic recombination rate coefficients for O^{3+} ($cm^3 s^{-1}$).

							log (*T*)									
λ (Å)	$2S'+1$	L'	$2S'+1$	L	E_i	E_k	3.0	3.2	3.4	3.6	3.8	4.0	4.2	4.4	4.6	4.8
15.599.4	−4	1	4	1	622 802	629 212	3.85 (−16)†	2.85 (−15)	7.81 (−15)	1.14 (−14)	1.13 (−14)	8.67 (−15)	5.70 (−15)	3.41 (−15)	1.92 (−15)	1.04 (−15)
9 188.8	−2	1	2	2	573 534	584 417	1.28 (−14)	9.15 (−15)	6.07 (−15)	3.81 (−15)	2.32 (−15)	1.42 (−15)	9.00 (−16)	6.20 (−16)	4.53 (−16)	3.28 (−16)
7 040.9	2	0	−2	1	485 570	499 773	1.41 (−15)	1.41 (−15)	1.70 (−15)	2.04 (−15)	2.48 (−15)	4.70 (−15)	9.06 (−15)	1.22 (−14)	1.21 (−14)	9.57 (−15)
5 508.8	4	2	−4	3	639 436	657 589	1.08 (−32)	2.87 (−25)	1.08 (−20)	6.44 (−18)	2.82 (−16)	2.37 (−15)	7.03 (−15)	1.08 (−14)	1.10 (−14)	8.63 (−15)
5 212.3	−2	1	2	1	609 075	628 260	5.67 (−15)	2.54 (−14)	5.06 (−14)	6.07 (−14)	5.27 (−14)	3.74 (−14)	2.34 (−14)	1.35 (−14)	7.37 (−15)	3.91 (−15)
5 140.1	4	3	−4	4	637 802	657 256	1.89 (−32)	3.98 (−25)	1.29 (−20)	7.02 (−18)	2.90 (−16)	2.35 (−15)	6.81 (−15)	1.03 (−14)	1.04 (−14)	8.12 (−15)
4 770.3	−4	1	4	2	606 354	627 317	8.30 (−15)	2.17 (−14)	3.08 (−14)	2.98 (−14)	2.27 (−14)	1.48 (−14)	8.85 (−15)	5.02 (−15)	2.78 (−15)	1.52 (−15)
4 659.6	−2	1	2	2	609 075	630 536	6.47 (−16)	9.66 (−15)	4.13 (−14)	8.01 (−14)	9.44 (−14)	8.11 (−14)	5.71 (−14)	3.55 (−14)	2.04 (−14)	1.11 (−14)
4 654.3	−2	3	2	4	636 068	657 553	1.78 (−32)	4.50 (−25)	1.64 (−20)	9.57 (−18)	4.13 (−16)	3.44 (−15)	1.02 (−14)	1.56 (−14)	1.59 (−14)	1.24 (−14)
4 632.3	2	4	−2	5	553 745	575 332	7.07 (−22)	7.12 (−22)	7.22 (−20)	2.10 (−18)	1.38 (−17)	3.67 (−17)	2.82 (−16)	6.23 (−15)	3.87 (−14)	9.54 (−14)
4 524.0	−4	4	4	5	635 254	657 358	2.09 (−32)	4.55 (−25)	1.51 (−20)	8.29 (−18)	3.45 (−16)	2.81 (−15)	8.17 (−15)	1.24 (−14)	1.25 (−14)	9.78 (−15)
4 374.8	−4	1	4	1	606 354	629 212	5.61 (−16)	4.15 (−15)	1.14 (−14)	1.67 (−14)	1.64 (−14)	1.26 (−14)	8.31 (−15)	4.96 (−15)	2.79 (−15)	2.51 (−15)
4 345.4	−2	3	2	4	552 240	575 254	2.13 (−15)	1.39 (−15)	8.29 (−16)	4.88 (−16)	3.16 (−16)	2.27 (−16)	2.66 (−16)	2.70 (−15)	1.60 (−14)	3.89 (−14)
4 292.4	−2	1	2	2	635 856	659 153	1.19 (−33)	7.11 (−26)	4.44 (−21)	3.65 (−18)	1.96 (−16)	1.87 (−15)	6.01 (−15)	9.74 (−15)	1.02 (−14)	8.18 (−15)
4 254.7	−4	2	4	3	602 794	626 297	6.83 (−14)	1.13 (−13)	1.21 (−13)	9.75 (−14)	6.61 (−14)	4.01 (−14)	2.27 (−14)	1.23 (−14)	6.54 (−15)	3.42 (−15)
4 203.8	−2	1	2	0	609 075	632 863	4.48 (−18)	2.32 (−16)	2.17 (−15)	6.90 (−15)	1.11 (−14)	1.16 (−14)	9.23 (−15)	6.20 (−15)	3.74 (−15)	2.10 (−15)
4 036.2	2	2	−2	3	599 853	624 629	1.48 (−12)	9.67 (−13)	5.73 (−13)	3.19 (−13)	1.71 (−13)	8.94 (−14)	4.60 (−14)	2.35 (−14)	1.19 (−14)	6.00 (−15)
3 756.9	2	2	−2	1	599 853	626 471	1.09 (−13)	1.88 (−13)	2.06 (−13)	1.69 (−13)	1.16 (−13)	7.08 (−14)	4.02 (−14)	2.18 (−14)	1.15 (−14)	5.93 (−15)
3 735.0	4	2	−4	3	468 323	495 096	3.08 (−12)	5.32 (−12)	6.01 (−12)	5.41 (−12)	4.38 (−12)	3.31 (−12)	2.32 (−12)	1.52 (−12)	9.52 (−13)	5.71 (−13)
3 551.6	2	4	−2	3	596 473	624 629	5.54 (−14)	3.62 (−14)	2.15 (−14)	1.20 (−14)	6.41 (−15)	3.35 (−15)	1.72 (−15)	8.79 (−16)	4.45 (−16)	2.25 (−16)
3 491.1	−2	1	2	2	518 447	547 091	2.84 (−13)	1.85 (−13)	1.10 (−13)	6.20 (−14)	3.44 (−14)	1.95 (−14)	1.20 (−14)	8.66 (−15)	6.92 (−15)	5.37 (−15)
3 410.2	−2	1	2	2	389 969	419 293	1.83 (−14)	1.20 (−14)	7.22 (−15)	4.26 (−15)	2.64 (−15)	1.81 (−15)	1.45 (−15)	1.38 (−15)	1.44 (−15)	1.43 (−15)
3 389.8	−4	1	4	2	438 823	468 323	3.26 (−12)	5.70 (−12)	6.64 (−12)	6.35 (−12)	5.53 (−12)	4.41 (−12)	3.21 (−12)	2.18 (−12)	1.41 (−12)	8.75 (−13)
3 352.8	−2	1	2	2	452 737	482 563	5.70 (−14)	3.74 (−14)	2.27 (−14)	1.41 (−14)	1.01 (−14)	7.95 (−15)	6.31 (−15)	4.99 (−15)	3.85 (−15)	2.79 (−15)
3 252.4	−2	1	2	1	597 514	628 260	2.43 (−15)	1.09 (−14)	2.17 (−14)	2.60 (−14)	2.26 (−14)	1.60 (−14)	1.00 (−14)	5.77 (−15)	3.16 (−15)	1.68 (−15)
3 199.8	−2	0	2	1	597 008	628 260	1.02 (−15)	4.57 (−15)	9.13 (−15)	1.10 (−14)	9.52 (−15)	6.76 (−15)	4.22 (−15)	2.43 (−15)	1.33 (−15)	7.07 (−16)
3 099.0	2	1	−2	1	594 202	626 471	2.64 (−14)	4.56 (−14)	5.00 (−14)	4.11 (−14)	2.82 (−14)	1.72 (−14)	9.76 (−15)	5.29 (−15)	2.79 (−15)	1.44 (−15)
3 065.8	2	0	−2	1	357 351	389 969	1.64 (−12)	1.10 (−12)	6.73 (−13)	4.00 (−13)	2.46 (−13)	1.65 (−13)	1.24 (−13)	1.07 (−13)	9.45 (−14)	7.78 (−14)
3 037.3	−2	3	2	4	624 629	657 553	1.24 (−32)	3.14 (−25)	1.14 (−20)	6.70 (−18)	2.90 (−16)	2.42 (−15)	7.14 (−15)	1.10 (−14)	1.11 (−14)	8.71 (−15)

3 028.3	−2	1	2	2	597 514	630 536	2.95 (−16)	4.42 (−15)	1.90 (−14)	3.68 (−14)	4.34 (−14)	3.73 (−14)	2.63 (−14)	1.63 (−14)	9.38 (−15)	5.12 (−15)
3 023.9	−2	1	2	2	514 022	547 091	1.09 (−14)	7.12 (−15)	4.23 (−15)	2.38 (−15)	1.32 (−15)	7.48 (−16)	4.60 (−16)	3.33 (−16)	2.66 (−16)	2.06 (−16)
2 906.1	−2	3	2	2	596 126	630 536	9.19 (−16)	1.37 (−14)	5.87 (−14)	1.14 (−13)	1.34 (−13)	1.15 (−13)	8.11 (−14)	5.04 (−14)	2.89 (−14)	1.58 (−14)
2 892.4	−4	2	4	3	591 724	626 297	5.78 (−13)	9.58 (−13)	1.02 (−12)	8.26 (−13)	5.60 (−13)	3.39 (−13)	1.92 (−13)	1.04 (−13)	5.53 (−14)	2.89 (−14)
2 744.4	−4	3	4	3	589 859	626 297	6.14 (−14)	1.02 (−13)	1.09 (−13)	8.78 (−14)	5.95 (−14)	3.61 (−14)	2.04 (−14)	1.10 (−14)	5.82 (−15)	3.02 (−15)
2 728.3	2	0	−2	1	589 817	626 471	5.57 (−14)	9.62 (−14)	1.05 (−13)	8.67 (−14)	5.93 (−14)	3.62 (−14)	2.06 (−14)	1.11 (−14)	5.87 (−17)	3.03 (−15)
2 672.2	−2	1	2	2	597 514	634 937	5.73 (−18)	8.91 (−16)	1.67 (−14)	8.20 (−14)	1.74 (−13)	2.16 (−13)	1.92 (−13)	1.39 (−13)	8.73 (−13)	5.05 (−14)
2 669.7	−4	3	4	2	589 859	627 317	5.53 (−14)	1.44 (−13)	2.05 (−13)	1.99 (−13)	1.51 (−13)	9.87 (−14)	5.89 (−14)	3.34 (−14)	1.85 (−14)	1.01 (−14)
2 633.3	−2	2	2	3	593 415	631 390	3.71 (−16)	8.69 (−15)	4.93 (−14)	1.14 (−13)	1.50 (−13)	1.39 (−13)	1.02 (−13)	6.54 (−14)	3.84 (−14)	2.13 (−14)
2 621.4	−4	1	4	2	593 107	631 255	4.27 (−16)	9.43 (−15)	5.15 (−14)	1.16 (−13)	1.51 (−13)	1.38 (−13)	1.10 (−13)	6.52 (−14)	3.87 (−14)	2.18 (−14)
2 528.4	4	4	−4	5	596 240	635 790	2.76 (−18)	6.23 (−16)	1.48 (−14)	8.43 (−14)	1.96 (−13)	2.59 (−13)	2.40 (−13)	1.78 (−13)	1.14 (−13)	6.73 (−14)
2 522.0	2	2	−2	3	596 247	635 897	8.38 (−19)	2.21 (−16)	5.76 (−15)	3.50 (−14)	8.46 (−14)	1.14 (−13)	1.07 (−13)	7.99 (−14)	5.14 (−14)	3.02 (−14)
2 516.5	−2	3	2	4	596 126	635 863	1.12 (−18)	2.72 (−16)	6.77 (−15)	3.99 (−14)	9.47 (−14)	1.27 (−13)	1.19 (−13)	9.02 (−14)	5.97 (−14)	3.63 (−14)
2 505.8	−4	1	4	1	438 823	478 731	5.33 (−14)	1.05 (−13)	1.74 (−13)	3.02 (−13)	4.29 (−13)	4.59 (−13)	4.06 (−13)	3.33 (−13)	2.58 (−13)	1.85 (−13)
2 486.8	2	2	−2	3	584 417	624 629	4.04 (−12)	2.64 (−12)	1.56 (−12)	8.71 (−13)	4.66 (−13)	2.44 (−13)	1.25 (−13)	6.39 (−14)	3.24 (−14)	1.63 (−14)
2 449.7	−2	3	2	4	512 922	553 745	1.22 (−15)	7.96 (−16)	4.75 (−16)	2.85 (−16)	1.99 (−16)	1.83 (−16)	1.51 (−15)	2.05 (−14)	9.16 (−14)	1.87 (−13)
2 408.8	4	3	−4	4	593 740	635 254	5.28 (−18)	9.72 (−16)	2.03 (−14)	1.07 (−13)	2.36 (−13)	3.03 (−13)	2.78 (−13)	2.09 (−13)	1.40 (−13)	8.61 (−14)
2 377.9	2	2	−2	1	584 417	626 471	2.46 (−13)	4.24 (−13)	4.64 (−13)	3.81 (−13)	2.61 (−13)	1.59 (−13)	9.04 (−14)	4.90 (−14)	2.58 (−14)	1.34 (−14)
1 945.3	2	1	−2	1	575 064	626 471	1.76 (−13)	3.04 (−13)	3.33 (−13)	2.74 (−13)	1.87 (−13)	1.14 (−14)	6.49 (−14)	3.52 (−14)	1.85 (−14)	9.57 (−15)
1 908.4	4	2	−4	3	580 151	632 550	1.28 (−16)	5.42 (−15)	4.48 (−14)	1.31 (−13)	2.01 (−13)	2.04 (−13)	1.60 (−13)	1.06 (−13)	6.41 (−14)	3.62 (−14)
1 827.3	−2	1	2	1	573 534	628 260	1.02 (−14)	4.55 (−14)	9.08 (−14)	1.09 (−13)	9.45 (−14)	6.71 (−14)	4.19 (−14)	2.41 (−14)	1.32 (−14)	7.01 (−15)
1 711.2	−4	1	4	2	568 877	627 317	3.40 (−14)	8.87 (−14)	1.26 (−13)	1.22 (−13)	9.28 (−14)	6.06 (−14)	3.62 (−14)	2.05 (−14)	1.14 (−14)	6.21 (−15)
1 355.1	−2	3	2	2	510 622	584 417	2.22 (−13)	1.59 (−13)	1.05 (−13)	6.59 (−14)	4.02 (−14)	2.46 (−14)	1.56 (−14)	1.07 (−14)	7.84 (−15)	5.68 (−15)
1 341.9	2	1	−2	2	180 388	254 908	3.34 (−13)	2.84 (−13)	3.34 (−13)	4.94 (−13)	6.56 (−13)	8.04 (−13)	9.46 (−13)	9.97 (−13)	8.94 (−13)	6.86 (−13)
1 300.6	2	1	−2	1	549 585	626 471	1.88 (−13)	3.24 (−13)	3.55 (−13)	2.92 (−13)	2.00 (−13)	1.22 (−13)	6.91 (−14)	3.75 (−14)	1.97 (−14)	1.02 (−14)
1 289.7	2	2	−2	3	547 091	624 629	1.71 (−11)	1.12 (−11)	6.61 (−12)	3.68 (−12)	1.97 (−12)	1 03 (−12)	5.30 (−13)	2.70 (−13)	1.37 (−13)	6.91 (−14)
1 242.5	2	2	−2	1	419 293	499 773	1.26 (−14)	1.27 (−14)	1.53 (−14)	1.83 (−14)	2.24 (−14)	4.23 (−14)	8.15 (−14)	1.10 (−13)	1.08 (−13)	8.61 (−14)
1 228.4	−2	1	2	2	518 447	599 853	1.26 (−13)	9.15 (−14)	6.24 (−14)	4.23 (−14)	3.11 (−14)	2.42 (−14)	1.81 (−14)	1.28 (−14)	8.98 (−15)	6.41 (−15)
1 080.0	−2	1	2	2	389 969	482 563	1.13 (−13)	7.40 (−14)	4.49 (−14)	2.79 (−14)	2.00 (−14)	1.57 (−14)	1.25 (−14)	9.87 (−15)	7.62 (−15)	5.52 (−15)
1 068.0	2	2	−2	3	419 293	512 922	1.64 (−14)	1.26 (−14)	1.44 (−14)	2.39 (−14)	3.67 (−14)	4.70 (−14)	5.42 (−14)	6.75 (−14)	9.10 (−14)	1.10 (−13)
1 062.2	−4	2	4	3	499 592	593 740	1.84 (−17)	1.00 (−15)	2.00 (−14)	1.04 (−13)	2.31 (−13)	2.99 (−13)	2.85 (−13)	2.30 (−13)	1.70 (−13)	1.16 (−13)
1 059.8	−2	1	2	2	452 737	547 091	7.79 (−13)	5.09 (−13)	3.02 (−13)	1.70 (−13)	9.43 (−14)	5.33 (−14)	3.28 (−14)	2.37 (−14)	1.90 (−14)	1.47 (−14)
1 046.0	−2	1	2	0	389 969	485 570	2.04 (−14)	3.44 (−14)	4.23 (−14)	6.23 (−14)	1.04 (−13)	1.45 (−13)	1.72 (−13)	1.81 (−13)	1.64 (−13)	1.28 (−13)
988.7	−4	3	4	4	495 096	596 240	1.71 (−17)	1.28 (−15)	2.09 (−14)	1.05 (−13)	2.33 (−13)	3.01 (−13)	2.77 (−13)	2.07 (−13)	1.36 (−13)	8.24 (−14)
922.5	2	1	−2	1	180 388	288 784	1.66 (−13)	2.06 (−13)	3.47 (−13)	6.15 (−13)	9.03 (−13)	1.18 (−12)	1.39 (−12)	1.40 (−12)	1.19 (−12)	8.74 (−13)

† 3.85 (−16) = 3.85×10^{-16}.

Table 3 (continued)

							log (T)									
λ (Å)	$2S'+1$	L'	$2S'+1$	L	E_i	E_k	3.0	3.2	3.4	3.6	3.8	4.0	4.2	4.4	4.6	4.8
789.4	−2	1	2	2	0	126 678	1.77 (−10)†	1.17 (−10)	7.17 (−11)	4.52 (−11)	3.17 (−11)	2.49 (−11)	2.14 (−11)	1.89 (−11)	1.60 (−11)	1.23 (−11)
789.2	−4	2	4	3	499 592	626 297	5.47 (−13)	9.07 (−13)	9.67 (−13)	7.81 (−13)	5.29 (−13)	3.21 (−13)	1.81 (−13)	9.84 (−14)	5.20 (−14)	2.71 (−14)
779.8	2	2	−2	2	126 678	254 908	1.91 (−12)	1.62 (−12)	1.91 (−12)	2.82 (−12)	3.74 (−12)	4.58 (−12)	5.40 (−12)	5.69 (−12)	5.11 (−12)	3.92 (−12)
762.2	−4	3	4	3	495 096	626 297	2.88 (−12)	4.78 (−12)	5.10 (−12)	4.12 (−12)	2.79 (−12)	1.69 (−12)	9.58 (−13)	5.20 (−13)	2.76 (−13)	1.44 (−13)
756.3	−4	3	4	2	495 096	627 317	1.94 (−13)	5.06 (−13)	7.20 (−13)	6.97 (−13)	5.30 (−13)	3.46 (−13)	2.07 (−13)	1.17 (−13)	6.49 (−14)	3.54 (−14)
747.2	2	0	−2	1	492 641	626 471	5.56 (−13)	9.59 (−13)	1.05 (−12)	8.63 (−13)	5.91 (−13)	3.60 (−13)	2.05 (−13)	1.11 (−13)	5.84 (−14)	3.02 (−14)
723.5	−4	2	4	3	499 592	637 802	3.48 (−19)	2.55 (−16)	1.27 (−14)	1.16 (−13)	3.61 (−13)	5.76 (−13)	6.02 (−13)	4.83 (−13)	3.30 (−13)	2.03 (−13)
703.9	2	2	−2	3	482 563	624 629	6.94 (−12)	4.53 (−12)	2.69 (−12)	1.50 (−12)	8.01 (−13)	4.19 (−13)	2.16 (−13)	1.10 (−13)	5.57 (−14)	2.81 (−14)
636.4	−2	1	2	2	389 969	547 091	8.72 (−12)	5.69 (−12)	3.38 (−12)	1.90 (−12)	1.06 (−12)	5.97 (−13)	3.67 (−13)	2.66 (−13)	2.12 (−13)	1.65 (−13)
625.5	4	1	−4	0	71 407	231 281	4.78 (−14)	3.46 (−13)	9.53 (−13)	1.43 (−12)	1.49 (−12)	1.23 (−12)	8.81 (−13)	5.86 (−13)	3.74 (−13)	2.30 (−13)
616.9	2	2	−2	1	126 678	288 784	3.82 (−13)	4.74 (−13)	7.98 (−13)	1.41 (−12)	2.08 (−12)	2.70 (−12)	3.19 (−12)	3.23 (−12)	2.74 (−12)	2.01 (−12)
609.3	−2	1	2	0	0	164 112	2.48 (−12)	2.23 (−12)	2.01 (−12)	2.15 (−12)	2.62 (−12)	2.96 (−12)	3.02 (−12)	2.91 (−12)	2.57 (−12)	2.01 (−12)
608.9	4	2	−4	3	468 323	632 550	4.39 (−16)	1.86 (−14)	1.54 (−13)	4.52 (−13)	6.91 (−13)	7.00 (−13)	5.48 (−13)	3.65 (−13)	2.20 (−13)	1.24 (−13)
554.4	−2	1	2	1	0	180 388	3.58 (−12)	5.58 (−12)	6.47 (−12)	6.51 (−12)	6.14 (−12)	5.62 (−12)	5.17 (−12)	4.71 (−12)	3.98 (−12)	3.03 (−12)
487.0	2	2	−2	3	419 293	624 629	6.08 (−12)	3.97 (−12)	2.35 (−12)	1.31 (−12)	7.02 (−13)	3.67 (−13)	1.89 (−13)	9.63 (−14)	4.88 (−14)	2.46 (−14)
442.8	2	0	−2	1	164 112	389 969	1.66 (−12)	1.11 (−12)	6.80 (−13)	4.04 (−13)	2.49 (−13)	1.67 (−13)	1.26 (−13)	1.08 (−13)	9.55 (−14)	7.87 (−14)
379.8	2	2	−2	1	126 678	389 969	5.80 (−12)	3.87 (−12)	2.38 (−12)	1.41 (−12)	8.71 (−13)	5.82 (−13)	4.39 (−13)	3.77 (−13)	3.34 (−13)	2.75 (−13)
342.3	−2	2	2	2	254 908	547 091	5.07 (−13)	3.31 (−13)	1.97 (−13)	1.11 (−13)	6.14 (−14)	3.48 (−14)	2.14 (−14)	1.55 (−14)	1.24 (−14)	9.59 (−15)
306.7	2	2	−2	1	126 678	452 737	7.78 (−13)	5.90 (−13)	4.76 (−13)	4.20 (−13)	3.67 (−13)	2.96 (−13)	2.28 (−13)	1.77 (−13)	1.36 (−13)	9.99 (−14)
291.2	−2	1	2	1	288 784	632 238	1.14 (−15)	4.53 (−14)	3.57 (−13)	1.02 (−12)	1.53 (−12)	1.54 (−12)	1.19 (−12)	7.88 (−13)	4.70 (−13)	2.64 (−13)
289.9	−2	2	2	2	254 908	599 853	1.10 (−12)	8.02 (−13)	5.47 (−13)	3.71 (−13)	2.73 (−13)	2.12 (−13)	1.58 (−13)	1.13 (−13)	7.88 (−14)	5.62 (−14)
288.9	−2	1	2	2	288 784	634 937	2.03 (−17)	3.16 (−15)	5.91 (−14)	2.91 (−13)	6.16 (−13)	7.67 (−13)	6.82 (−13)	4.91 (−13)	3.09 (−13)	1.79 (−13)
279.8	−2	1	2	0	0	357 351	1.85 (−12)	1.28 (−13)	8.28 (−13)	5.34 (−13)	3.69 (−13)	3.12 (−13)	3.36 (−13)	3.66 (−13)	3.43 (−13)	2.76 (−13)
279.5	−2	1	2	2	288 784	646 625	5.10 (−24)	3.94 (−19)	3.70 (−16)	2.16 (−14)	2.17 (−13)	7.22 (−13)	1.20 (−12)	1.27 (−12)	1.03 (−12)	6.95 (−13)
274.4	−2	1	2	2	288 784	653 170	2.75 (−28)	6.89 (−22)	5.82 (−18)	1.35 (−15)	3.27 (−14)	1.89 (−13)	4.42 (−13)	5.87 (−13)	5.44 (−13)	4.01 (−13)
272.2	4	1	−4	1	71 407	438 823	3.44 (−12)	6.18 (−12)	7.47 (−12)	7.46 (−12)	6.75 (−12)	5.52 (−12)	4.09 (−12)	2.86 (−12)	1.91 (−12)	1.23 (−12)
266.9	2	2	−2	2	126 678	501 283	7.48 (−14)	1.87 (−13)	4.16 (−13)	6.87 (−13)	8.41 (−13)	8.08 (−13)	6.66 (−13)	5.07 (−13)	3.65 (−13)	2.47 (−13)
265.6	−2	2	2	3	254 908	631 390	3.55 (−15)	8.30 (−14)	4.70 (−13)	1.09 (−12)	1.43 (−12)	1.32 (−12)	9.74 (−13)	6.23 (−13)	3.66 (−13)	2.03 (−13)
264.9	−2	2	2	3	254 908	632 466	4.79 (−16)	2.12 (−14)	1.80 (−13)	5.38 (−13)	8.31 (−13)	8.49 (−13)	6.71 (−13)	4.53 (−13)	2.78 (−13)	1.61 (−13)
260.5	2	2	−2	3	126 678	510 622	2.69 (−13)	2.16 (−13)	2.77 (−13)	4.78 (−13)	6.80 (−13)	7.57 (−13)	7.21 (−13)	6.37 (−13)	5.47 (−13)	4.51 (−13)

255.3	−2	2	2	2	254 908	646 625	4.75 (−24)	3.67 (−19)	3.45 (−16)	2.01 (−14)	2.02 (−13)	6.74 (−13)	1.11 (−12)	1.19 (−12)	9.58 (−13)	6.48 (−13)
254.1	−2	2	2	3	254 908	648 436	1.72 (−25)	3.46 (−20)	5.96 (−17)	5.08 (−15)	6.51 (−14)	2.52 (−13)	4.60 (−13)	5.21 (−13)	4.38 (−13)	3.05 (−13)
251.3	−4	0	4	1	231 281	629 212	4.62 (−14)	3.42 (−13)	9.39 (−13)	1.38 (−12)	1.36 (−12)	1.04 (−12)	6.87 (−13)	4.10 (−13)	2.31 (−13)	1.25 (−13)
251.1	−2	2	2	2	254 908	653 170	3.95 (−28)	9.91 (−22)	8.37 (−18)	1.95 (−15)	4.70 (−14)	2.72 (−13)	6.36 (−13)	8.44 (−13)	7.82 (−13)	5.77 (−13)
249.0	−2	2	2	3	254 908	656 487	2.87 (−30)	4.19 (−23)	1.08 (−18)	5.05 (−16)	1.90 (−14)	1.45 (−13)	4.05 (−13)	6.00 (−13)	5.96 (−13)	4.60 (−13)
238.5	−2	1	2	2	0	419 293	6.11 (−12)	4.00 (−12)	2.41 (−12)	1.42 (−12)	8.80 (−13)	6.04 (−13)	4.84 (−13)	4.61 (−13)	4.80 (−13)	4.76 (−13)
233.5	4	1	−4	2	71 407	499 592	5.82 (−13)	1.04 (−12)	1.29 (−12)	1.39 (−12)	1.52 (−12)	1.53 (−12)	1.35 (−12)	1.06 (−12)	7.73 (−13)	5.24 (−13)
224.2	2	1	−2	1	180 388	626 471	2.74 (−12)	4.73 (−12)	5.18 (−12)	4.25 (−12)	2.91 (−12)	1.78 (−12)	1.01 (−12)	5.46 (−13)	2.88 (−13)	1.49 (−13)
220.5	2	1	−2	2	180 388	633 978	4.72 (−17)	4.43 (−15)	6.03 (−14)	2.43 (−13)	4.53 (−13)	5.21 (−13)	4.41 (−13)	3.08 (−13)	1.91 (−13)	1.09 (−13)
216.3	2	0	−2	1	164 112	626 471	4.56 (−13)	7.87 (−13)	8.63 (−13)	7.09 (−13)	4.85 (−13)	2.96 (−13)	1.68 (−13)	9.11 (−14)	4.80 (−14)	2.48 (−14)
212.0	2	0	−2	1	164 112	635 856	1.09 (−17)	2.75 (−15)	7.01 (−14)	4.19 (−13)	1.00 (−12)	1.35 (−12)	1.26 (−12)	9.36 (−13)	6.01 (−13)	3.53 (−13)
207.2	−2	1	2	2	0	482 563	6.60 (−12)	4.33 (−12)	2.63 (−12)	1.64 (−12)	1.17 (−12)	9.20 (−13)	7.30 (−13)	5.78 (−13)	4.46 (−13)	3.23 (−13)
203.0	−2	1	2	0	0	492 641	4.86 (−13)	8.40 (−13)	9.29 (−13)	7.97 (−13)	6.06 (−13)	4.37 (−13)	3.10 (−13)	2.20 (−13)	1.52 (−13)	1.00 (−13)
200.8	2	2	−2	3	126 678	624 629	1.68 (−10)	1.09 (−10)	6.48 (−11)	3.61 (−11)	1.93 (−11)	1.01 (−11)	5.20 (−12)	2.65 (−12)	1.34 (−12)	6.78 (−13)
197.1	2	2	−2	2	126 678	633 978	5.99 (−17)	5.63 (−15)	7.66 (−14)	3.08 (−13)	5.75 (−13)	6.61 (−13)	5.60 (−13)	3.91 (−13)	2.42 (−13)	1.39 (−13)
196.3	2	2	−2	3	126 678	636 068	1.39 (−17)	3.93 (−15)	1.08 (−13)	6.74 (−13)	1.66 (−12)	2.28 (−12)	2.15 (−12)	1.61 (−12)	1.04 (−12)	6.10 (−13)
196.2	2	2	−2	1	126 678	636 454	2.24 (−18)	7.79 (−16)	2.42 (−14)	1.64 (−13)	4.27 (−13)	6.03 (−13)	5.82 (−13)	4.41 (−13)	2.86 (−13)	1.69 (−13)
192.2	4	1	−4	2	71 407	591 724	5.32 (−13)	9.04 (−13)	1.02 (−12)	9.02 (−13)	7.00 (−13)	5.04 (−13)	3.48 (−13)	2.37 (−13)	1.60 (−13)	1.05 (−13)
188.4	2	2	−2	3	126 678	657 509	8.89 (−31)	2.20 (−23)	7.91 (−19)	4.59 (−16)	1.97 (−13)	1.64 (−13)	4.84 (−13)	7.42 (−13)	7.53 (−13)	5.89 (−13)
185.1	2	2	−2	3	126 678	667 033	1.16 (−36)	4.55 (−27)	3.99 (−21)	1.74 (−17)	2.66 (−15)	4.93 (−14)	2.41 (−13)	5.09 (−13)	6.31 (−13)	5.61 (−13)
182.8	−2	1	2	2	0	547 091	6.73 (−12)	4.40 (−12)	2.61 (−12)	1.47 (−12)	8.15 (−13)	4.61 (−13)	2.84 (−13)	2.05 (−13)	1.64 (−13)	1.27 (−13)
177.8	4	1	−4	2	71 407	633 808	4.80 (−16)	4.18 (−14)	5.43 (−13)	2.13 (−12)	3.90 (−12)	4.43 (−12)	3.72 (−12)	2.59 (−12)	1.60 (−12)	9.15 (−13)
177.7	4	1	−4	1	71 407	634 092	5.96 (−17)	5.89 (−15)	8.28 (−14)	3.40 (−13)	6.43 (−13)	7.45 (−13)	6.36 (−13)	4.49 (−13)	2.82 (−13)	1.65 (−13)
171.1	−2	1	2	2	0	584 417	3.06 (−12)	2.18 (−12)	1.45 (−12)	9.08 (−13)	5.54 (−13)	3.39 (−13)	2.15 (−13)	1.48 (−13)	1.08 (−13)	7.82 (−14)
159.2	−2	1	2	1	0	628 260	2.19 (−13)	9.80 (−13)	1.96 (−12)	2.34 (−12)	2.04 (−12)	1.45 (−12)	9.02 (−13)	5.20 (−13)	2.85 (−13)	1.51 (−13)
158.6	−2	1	2	2	0	630 536	2.12 (−14)	3.16 (−13)	1.35 (−12)	2.62 (−12)	3.09 (−12)	2.65 (−12)	1.87 (−12)	1.16 (−12)	6.65 (−13)	3.63 (−13)

	$2S+1$	L	$2J$	E_j	3.0	3.2	3.4	3.6	3.8	4.0	4.2	4.4	4.6	4.8
	−2	1	1	0	7.50 (−11)	5.03 (−11)	3.29 (−11)	2.29 (−11)	1.75 (−11)	1.42 (−11)	1.19 (−11)	1.02 (−11)	8.40 (−12)	6.42 (−12)
	−2	1	3	380	1.34 (−10)	9.32 (−11)	6.21 (−11)	4.35 (−11)	3.34 (−11)	2.76 (−11)	2.41 (−11)	2.15 (−11)	1.82 (−11)	1.41 (−11)
	4	1	1	71 441	4.27 (−13)	9.04 (−13)	1.37 (−12)	1.76 (−12)	1.94 (−12)	1.80 (−12)	1.50 (−12)	1.23 (−12)	9.70 (−13)	7.13 (−13)
	4	1	3	71 573	1.24 (−12)	2.36 (−12)	3.23 (−12)	3.90 (−12)	4.23 (−12)	3.92 (−12)	3.21 (−12)	2.47 (−12)	1.84 (−12)	1.28 (−12)
	4	1	5	71 791	3.03 (−12)	5.51 (−12)	7.17 (−12)	8.53 (−12)	9.42 (−12)	8.92 (−12)	7.31 (−12)	5.52 (−12)	3.96 (−12)	2.68 (−12)

† 1.77 (−10) = 1.77×10^{-10}.

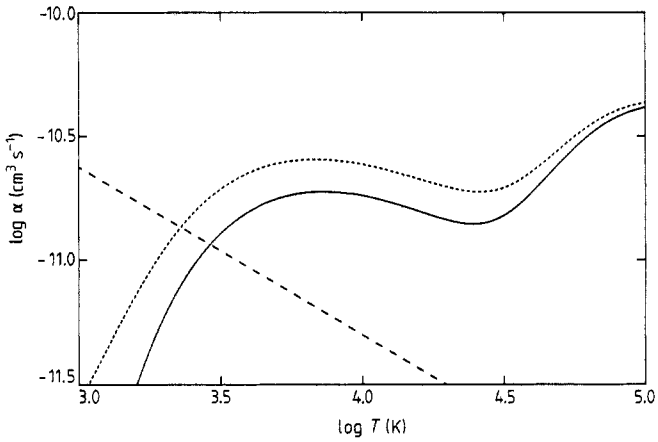

Figure 2. Total recombination rate coefficients for N^{2+}. ——, *LS*-coupling dielectronic recombination, this work; - - -, intermediate-coupling dielectronic recombination, this work; - - -, direct radiative recombination, Aldrovandi and Péquignot (1976).

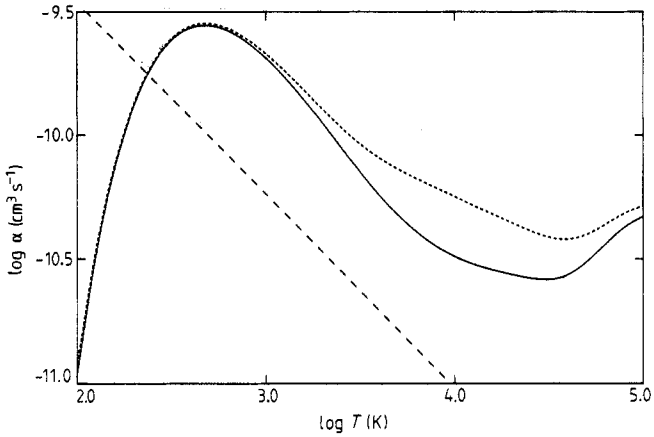

Figure 3. Total recombination rate coefficients for O^{3+}. ——, *LS*-coupling dielectronic recombination, this work; - - - -, intermediate-coupling dielectronic recombination, this work; - - -, direct radiative recombination, Aldrovandi and Péquignot (1973).

and intermediate-coupling results for α_d(tot) and also display the total direct radiative recombination rate coefficient evaluated from the fit given by Aldrovandi and Péquignot (1973, 1976).

5.1. $\alpha_d^*(j)$ and $\alpha_d^*(h \to j)$

Large numbers of effective dielectronic recombination rate coefficients are generated by the intermediate-coupling calculation. In order to keep them down to a manageable number we only present results for the quartet-quartet transition lines and selected doublet-doublet lines summed over J, J' according to

$$\alpha_d^*(\Gamma SL \to \Gamma' S' L') = \sum_{J,J'} \alpha_d^*(\Gamma SLJ \to \Gamma' S' L' J') \tag{5.1}$$

with eigenenergies averaged according to

$$E(\Gamma SL) = \frac{\Sigma_J\,(2J+1)E(\Gamma SLJ)}{\Sigma_J\,(2J+1)} \tag{5.2}$$

and given in units of cm^{-1} relative to the ground term with the emitted photon wavelength λ in Å. Furthermore, only those lines that satisfy $\alpha_d^*(\Gamma SL \rightarrow \Gamma' S' L') > A_0$ at some point in the temperature range $T = 10^3$-6.3×10^4 K are included. Where A_0 is given by $A_0(C^+) = 10^{-14}$ cm^3 s^{-1}; $A_0(N^{2+}) = 10^{-14}$, 5×10^{-14} and 10^{-13} cm^3 s^{-1} for $\lambda >$ 3000 Å, 3000 Å $\geq \lambda \geq$ 912 Å and $\lambda <$ 912 Å respectively and $A_0(O^{3+}) = 10^{-14}$, 10^{-13} and 5×10^{-13} cm^3 s^{-1} for the same wavebands. Finally, a negative spin multiplicity denotes odd parity.

Comprehensive tables of results for $\alpha_d^*(\Gamma SL \rightarrow \Gamma' S' L')$ and $\alpha_d^*(\Gamma SLJ \rightarrow \Gamma' S' L' J')$ are available from the author (Badnell 1987b) for both doublet-doublet and quartet-quartet transitions.

Contributions to the effective dielectronic recombination rate coefficients from the $2s2p(^3P)nl$ autoionising levels with $n > n_0$ were evaluated using the n^{-3} scaling behaviour of the transition rates as described in detail by Nussbaumer and Storey (1983) and Badnell (1987a). This extrapolation only contributes at the highest temperatures we consider. At $T = 6.3 \times 10^4$ K it contributes about 20% of the $\alpha_d^*(j)$ given in tables 1-3 and it falls off rapidly with decreasing temperature. Contributions from $2s2p(^1P)nl$ levels with $n > n_0$ can only be evaluated for α_d(tot), see § 5.2. These levels have little or no affect on the α_d^* quartets since doublet-quartet radiative rates are negligible; however, this is not the case for the doublet $\alpha_d^*(j)$: their rising contribution to α_d(tot) with T can be seen in figures 1-3. They contribute approximately 20% of the doublet contribution to α_d(tot) for C^+, N^{2+} and O^{3+} at $T = 2.0$, 3.0 and 4.0×10^4 K respectively. Thus, the values of $\alpha_d^*(^2P_J)$ for the $J = \frac{1}{2}$ and $J = \frac{3}{2}$ levels of the ground term should be considered an underestimate above these temperatures. As shown by equation (2.1), the rate of population of the ground and metastable levels is proportional to $\alpha_d^*(j)$. As expected, the ratio of $\alpha_d^*(^2P_{3/2})$ to $\alpha_d^*(^2P_{1/2})$ is equal to the ratio of their statistical weights to within 10% at $T = 6 \times 10^4$ K. This is not so for the ^4P_J metastable levels, see tables 1-3.

Direct radiative recombination also populates the $2s^2nl\ ^2L_J$ levels and must be included for recombination lines arising from these levels.

5.1.1. C^+ and N^{2+}. Our *LS*-coupling results for effective dielectronic recombination line coefficients (Badnell 1987b) agree to within about 10% with those of Nussbaumer and Storey (1984, table II*a*) for C^+ and about 20% for N^{2+} (Nussbaumer and Storey 1984 table VI*a*) except for three lines, see below. Our intermediate-coupling results agree to 10% and better with our *LS*-coupling results except for those lines enhanced by transitions from levels forbidden to autoionise in *LS* coupling due to parity conservation, in particular the N^{2+} $\lambda = 685.7$ Å line coefficient is increased by a factor of two. These new lines and enhanced lines for doublet-doublet transitions are given in table 1 and 2 along with the two strongest *LS*-allowed lines.

It is of interest to look more closely at the three lines of N^{2+} for which our *LS*-coupling results differ markedly from those of Nussbaumer and Storey (1984). Their $\lambda = 4477.8$ Å $^2H^\circ \rightarrow {}^2G$ line coefficient is a factor of six larger than our result, which is still too weak to appear in table 2 in intermediate coupling. Our radiative rate for $^2H^\circ \rightarrow {}^2G$ differs by less than 10% from that calculated by Nussbaumer and Storey (1984), but our autoionisation rate (the inverse of which populates $^2H^\circ$) is a

factor of ten smaller than the radiative rate so $\alpha_d^*(^2H^\circ \rightarrow {}^2G)$ is sensitive to errors in A_a. Nussbaumer and Storey (1984) evaluated A_a from the threshold value of the excitation collision strength for the parent terms since in general $A_a^{LS} \gg A_r^{LS}$ and great accuracy is not required for A_a^{LS}. However, A_a^{LS} falls off with increasing L. It would appear then that Nussbaumer and Storey's result for this line is an overestimate. The two sets of *LS* coupling results for the N^{2+} $\lambda = 6938$ and $\lambda = 2199$ Å lines differ by a factor two and four respectively, as do the radiative rates for these transitions. The only difference between our configuration expansions is our use of correlation configurations. It would appear that these affect the line strengths for these transitions. Our results may be an improvement but could still be subject to large errors (see § 5.2.2).

Nussbaumer and Storey (1984) applied their WI approximation to the parity-forbidden autoionising terms of N^{2+}. Their results (Nussbaumer and Storey 1984, table XIII) are very much an overestimate as they warned they might be. For example, they are a factor of seven larger than our intermediate-coupling results (table 2) for the $\lambda = 1908$ Å line, which does not exist in *LS* coupling. Also, the $\lambda = 991.0$ and 979.9 Å line coefficients are overestimated by factors of two and four respectively. These two lines are much better described by Nussbaumer and Storey's (1984) original results. The core fine-structure interactions are not strong enough for their WI approximation to be applicable.

The quartet-quartet lines of C^+ are generally weak compared with the doublet-doublet lines but the N^{2+} quartet-quartet lines are much stronger and a number of them are comparable to all but the strongest two doublet-doublet lines.

5.1.2. O^{3+}. Nussbaumer and Storey's (1984) table XI*a* of *LS*-coupling results for this ion contain transitions from ^2F terms that are forbidden to autoionise in *LS* coupling. It would appear that they have used their WI approximation for the $2s2p5f\,^2F$ term at 631 575 cm^{-1} and the $2p^23d\,^2F$ term at 641 535 cm^{-1} since there is no population by dielectronic capture and radiative transitions from higher levels have little effect (see § 5.3). Comparison with our intermediate-coupling results in table 3 again shows the WI results to be very much an overstimate, typically by a factor of four or five. Furthermore, cascades from these terms give rise to overestimates for a number of other lines, although some of this is compensated for in our intermediate-coupling calculation by cascades from other *LS*-forbidden doublets. Similar arguments apply to Nussbaumer and Storey's (1984) WI results for O IV in their table XIII, presumably for all parity-forbidden terms now. Because of these uncertainties and those discussed previously for N^{2+} we tabulate all of our doublet-doublet intermediate-coupling lines for O^{3+} that satisfy the same criterion for inclusion as the quartet-quartet lines (see § 5.1).

5.2. $\alpha_d(tot)$

At the highest temperature tabulated in table 4 our results for $\alpha_d(\text{tot})$ differ by only a few per cent from our previous *LS*-coupling results which extend to much higher temperatures (see Badnell 1987a). Contributions to $\alpha_d(\text{tot})$ from the $2s2p(^1P)nl$ autoionising levels with $n > n_0$ were evaluated in *LS* coupling as described in Badnell (1987a)—as there is no core fine-structure in this case, contributions from the $2s2p(^3P)nl$ levels were evaluated as in § 5.1.

5.2.1. C^+ and N^{2+}. Nussbaumer and Storey (1983, 1984) gave fits to their *LS*-coupling results for $\alpha_d(\text{tot})$ and these lie 10% above our results for C^+ at $T = 3.5 \times 10^3$ K and

Table 4. Total dielectronic recombination rate coefficients ($cm^3\ s^{-1}$).

C^+		N^{2+}		O^{3+}			
log T (K)	α_d(tot)	log T (K)	α_d(tot)	log T (K)	α_d(tot)	log T (K)	α_d(tot)
3.0	2.85 (−12)†	3.0	2.66 (−12)	2.2	7.65 (−11)	4.0	5.64 (−11)
3.2	6.67 (−12)	3.2	7.23 (−12)	2.4	1.95 (−10)	4.2	4.79 (−11)
3.4	9.65 (−12)	3.4	1.53 (−11)	2.6	2.76 (−10)	4.4	4.11 (−11)
3.6	9.86 (−12)	3.6	2.25 (−11)	2.8	2.70 (−10)	4.6	3.79 (−11)
3.8	8.07 (−12)	3.8	2.54 (−11)	3.0	2.13 (−10)	4.8	4.36 (−11)
4.0	6.05 (−12)	4.0	2.43 (−11)	3.2	1.52 (−10)	5.0	5.17 (−11)
4.2	4.96 (−12)	4.2	2.12 (−11)	3.4	1.07 (−10)	5.2	5.05 (−11)
4.4	7.15 (−12)	4.4	1.88 (−11)	3.6	8.06 (−11)	5.4	4.02 (−11)
4.6	1.66 (−11)	4.6	2.28 (−11)	3.8	6.65 (−11)	5.6	2.74 (−11)
4.8	2.82 (−11)	4.8	3.48 (−11)				
5.0	3.19 (−11)	5.0	4.32 (−11)				
5.2	2.69 (−11)	5.2	4.04 (−11)				

† 2.85 (−12) = 2.85×10^{-12}.

15% above our results for N^{2+} at $T = 8\times10^3$ K. Our intermediate-coupling results for α_d(tot) for C^+ are 12% greater than our *LS*-coupling results at $T = 3.5\times10^3$ K, and for N^{2+} they are 35% greater at $T = 8\times10^3$ K. This is due to the increase in the strength of the core fine-structure interactions as the charge on the ion increases. The ratio α_d^{IC}(tot)/α_d^{LS}(tot) can be made as large as we like by decreasing T since the first two (six) terms above the 2^1S ionisation limit of C^{2+} (N^{3+}) are forbidden to autoionise in *LS* coupling. Of course, direct radiative recombination may be dominant by then.

5.2.2. O^{3+}. O^{3+} is a rather different case and it has been discussed in detail by Nussbaumer and Storey (1983). The first autoionising term, $2p^2(^1D)3p\ ^2F°$, lies only 494 cm^{-1} above the O^{4+} 2^1S ionisation limit (see Moore 1983) and it is *LS* allowed. However, the position of this term is poorly determined by SUPERSTRUCTURE and so is the line strength for the (dominant) stabilising radiative transition to $2s2p^2\ ^2D$. Nussbaumer and Storey (1983) thus used the radiative rate determined from the photoionisation cross section that they had evaluated from the close-coupling code IMPACT. Nussbaumer and Storey (1983) found this value to be about a factor of three smaller than their SUPERSTRUCTURE result. Due to our use of correlation configurations we obtain an overestimate of a factor of two, better but not good enough, and so we reduce our radiative rates for this transition by a factor of two. Our *LS*-coupling results for α_d(tot) thus agree to within 10% with those of Nussbaumer and Storey (1983) over $T = 10^3$-6×10^4 K. However, at $T = 10^4$ K the results of Nussbaumer and Storey (1984) lie 25% above their 1983 results due to the inclusion of ^{2}F parity-forbidden autoionising terms as discussed above (§ 5.1.2). Finally, our intermediate-coupling results for α_d(tot) are 70% greater than our *LS*-coupling results at $T = 10^4$ K.

5.3. Radiative transitions between autoionising levels

We assume that the autoionising levels are populated by dielectronic capture and by radiative cascade from all higher levels included explicitly in the calculation as well as by radiative transitions from levels of the $2s2p(^3P)nl$ ($n > n_0$) configurations, which

in turn are assumed to be populated solely by dielectronic capture as extrapolated from $n = n_0$. The net result of including these radiative transitions is to increase $\alpha_d^{IC}(\text{tot})$ by less than 2% at $T = 6 \times 10^4$ K. However, if we consider the quartets separately we find that the increase is about 10% at $T = 6 \times 10^4$ K but falls off rapidly with decreasing temperature. This effect is included in our results for the effective dielectronic recombination rate coefficients given in tables 1-3.

In *LS* coupling, radiative transitions between autoionising terms are the sole method of population of the $^2S^\circ$, $^2D^\circ$, ... and ^2P, ^2F, ... terms that lie between the 2^1S_0 and 2^3P_0 ionisation limits and it results in an increase in $\alpha_d^{LS}(\text{tot})$ of less than 1% at $T = 6 \times 10^4$ K, while the individual effective dielectronic recombination lines are much too weak to satisfy $\alpha_d^*(j \to h) > A_0$ as defined above (§ 5.1).

6. Conclusion

We have looked at the effect of including core fine-structure interactions on dielectronic recombination at low temperatures. As the ion charge increases these interactions become stronger leading to stronger quartet-quartet lines (compare the results for C^+ and N^{2+}) but the effect on $\alpha_d(\text{tot})$ also depends on whether the lowest autoionising levels are *LS* allowed or *LS* forbidden as in the case of O^{3+}. However, the interactions are not strong enough for the WI approximation of Nussbaumer and Storey (1984) to be applicable. Errors in the structure can give rise to uncertainties in the transition rates and in addition, in intermediate coupling, to errors in the mixing of *LS*-allowed and *LS*-forbidden autoionising levels. It is also important to know the precise positions of the lowest autoionising levels relative to the ionisation limit. The reason we have not continued with the B-like sequence is that there is no observed data on any of the autoionising levels, and for Ne^{5+}, for example, it is not even possible to tell from our structure calculations which of the levels that lie close to the Ne^{6+} 2^1S ionisation limit are in fact autoionising and which are truly bound.

It is important that other sequences be investigated. Comparison of the number of radiative channels accessible in *LS* coupling and intermediate coupling gives a rough guide to the possible importance of core fine-structure interactions. But the key points are the actual strength of the core fine-structure interactions relative to the ratios A_a^{LS}/A_r^{LS} for a given ion and the relative positions of the lowest *LS*-allowed and *LS*-forbidden autoionising levels, as investigated by Nussbaumer and Storey in their WI approximation. Their results indicate that the Be-like (B-like), O-like, Mg-like and Al-like recombined sequences should be the subject of further intermediate-coupling calculations.

Acknowledgments

I would like to thank Dr Alan Burgess for his continued interest throughout this research program which has been funded by the SERC.

References

Aldrovandi S M V and Péquignot D 1973 *Astron. Astrophys.* **25** 137-40 (and erratum 1976 *Astron. Astrophys.* **47** 321)

Badnell N R 1985 *Cambridge Department of Applied Mathematics and Theoretical Physics, Report DAMTP/AA/-1001-NRB*
—— 1986 *J. Phys. B: At. Mol. Phys.* **19** 3827-35
—— 1987a *J. Phys. B: At. Mol. Phys.* **20** 2081-90
—— 1987b *Cambridge Department of Applied Mathematics and Theoretical Physics, Report DAMTP/AA/-1002-NRB*
Beigman I L and Chichkov B N 1980 *J. Phys. B: At. Mol. Phys.* **13** 565-9
Bethe H A and Salpeter E E 1977 *Quantum Mechanics of one and two-electron atoms* (New York: Plenum)
Blume M and Watson R E 1962 *Proc. R. Soc.* A **270** 127-43
Burgess A 1964 *Astrophys. J.* **139** 776-80
—— 1966 *Auto-ionization* ed A Temkin (Baltimore: Mono) pp 25-31
Eissner W, Jones M and Nussbaumer H 1974 *Comput. Phys. Commun.* **8** 270-306
Harrington J P, Lutz J H, Seaton M J and Stickland D J 1980 *Mon. Not. R. Astron. Soc.* **191** 13-22
Jones M 1970 *J. Phys. B: At. Mol. Phys.* **3** 1571-92
—— 1971 *J. Phys. B: At. Mol. Phys* **4** 1422-39
Moore C E 1970 *Atomic Energy Levels* NSRDS-NBS3, section 3 (Washington, DC: US Govt Printing Office)
—— 1975 *Atomic Energy Levels* NSRDS-NBS3, section 5 (Washington, DC: US Govt Printing Office)
—— 1983 *Atomic Energy Levels* NSRDS-NBS3, section 11 (Washington, DC: US Govt Printing Office)
Nussbaumer H and Storey P J 1978 *Astron. Astrophys.* **64** 139-44
—— 1981 *Astron. Astrophys.* **96** 91-5
—— 1983 *Astron. Astrophys.* **126** 75-9
—— 1984 *Astron. Astrophys. Suppl. Ser.* **56** 293-312
—— 1986 *Astron. Astrophys. Suppl. Ser.* **64** 545-55
—— 1987 *Astron. Astrophys. Suppl. Ser.* **69** 123-33
Storey P J 1981 *Mon. Not. R. Astron. Soc.* **195** 27-31P
Zeippen C J, Seaton M J and Morton D C 1977 *Mon. Not. R. Astron. Soc.* **181** 527-40